

Influence of bismuth on properties and microstructures of $\text{Sr}_{0.5}\text{Ba}_{0.5-x}\text{Bi}_x\text{TiO}_3$ thin films

TAO WENHONG, WANG YIN[†], FU XINGHUA* and WEI QIHONG

Department of Materials Science and Engineering, [†]Department of Foreign Languages, Jinan University, Jinan 250022, PR China

MS received 3 December 2005; revised 9 August 2006

Abstract. The influence of bismuth (Bi) on the dielectric and ferroelectric properties of $\text{Sr}_{0.5}\text{Ba}_{0.5-x}\text{Bi}_x\text{TiO}_3$ (BST, $0 \leq x \leq 0.030$ mol) thin films was studied. The results showed that the dielectric constant (ϵ_r) and dielectric loss ($\tan \delta$) decreased, and temperature, T_m , for maximum ϵ_r (Curie temperature), moved to lower temperature with increasing Bi content. The P_r , P_s and E_c were $0.22 \mu\text{C}/\text{cm}^2$, $0.32 \mu\text{C}/\text{cm}^2$ and $60 \text{ kV}/\text{cm}$, respectively for $\text{Sr}_{0.5}\text{Ba}_{0.485}\text{Bi}_{0.015}\text{TiO}_3$ thin films measured at 100 Hz, 20 V. The microstructure of BST thin films was studied by XRD and TEM. Tetragonal perovskite grains existed in BST thin films, but the grain size decreased with increasing doping ratio in BST. The characteristic absorption band for octahedron [TiO_2] (471.65 cm^{-1}) was shifted to lower wave number.

Keywords. BST thin films; dielectric constant; dielectric loss; Bi dopant; characteristic microstructure.

1. Introduction

(Ba, Sr) TiO_3 (BST) solid solution has good electrical properties, because the characteristics of BaTiO_3 (BT) is of high dielectric constant, and the characteristics of SrTiO_3 (ST) is of stable microstructure and low dielectric loss. Recent studies indicate that $\text{Sr}_{1-x}\text{Ba}_x\text{TiO}_3$ thin films with high dielectric constant, low leakage current, good dielectric-temperature characteristics and tunability of Curie temperature with ratio, Ba/Sr, are very promising materials for application in dynamic random access memory (DRAM) (Kotecki *et al* 1999; Mandeliman *et al* 2002), pyroelectric detectors, tunable microwave devices, phase shifters, electroluminescence display etc (Liou and Chiou 1997; Liu *et al* 2000). So, $\text{Sr}_{1-x}\text{Ba}_x\text{TiO}_3$ films have gained increasing interest in the investigation and fabrication of thin films. The exploitation of BST thin films for applications in nonvolatile memory of high memory rate and density, and tunable microwave device of high performance (Erker *et al* 2000), has been an important aspect of studies on thin films. So far no studies on Bi doped in $\text{Sr}_{1-x}\text{Ba}_x\text{TiO}_3$ thin films have been reported and here we report our results of investigation on $\text{Sr}_{0.5}\text{Ba}_{0.5-x}\text{Bi}_x\text{TiO}_3$ thin films.

2. Experimental

2.1 Materials

Chemical reagents, strontium acetate ($\text{Sr}(\text{CH}_3\text{COO})_2 \cdot 1/2\text{H}_2\text{O}$), bismuth nitrate ($\text{Bi}(\text{NO}_3)_3$), barium acetate ($\text{Ba}(\text{CH}_3\text{COO})_2$),

and titanium tetrabutoxide ($\text{Ti}(\text{OC}_4\text{H}_9)_4$), were used as source materials of strontium, bismuth, barium and titanium, respectively, and acetate acid and ethanol as solvents, acetylacetone and glycerin as chelating and surface activation agents, respectively.

2.2 Instruments

Phase composition of the prepared films was characterized by X-ray diffractometry (D/max-rA, Japan $\text{CuK}\alpha$, $\lambda = 0.15406 \text{ nm}$). Morphologies of the films were observed using transmission electron microscope (JEM-2010, Japan), and infrared analyser (FTS165, USA). Performance of the films was tested by HP Agilent 4294 A impedance analyser (frequency from 40 Hz–110 MHz), wide frequency LCR digital bridge, TH2816 and hysteresis loop instrumentation, TFA analyser 2000 (Germany).

2.3 Thin films preparation

$\text{Sr}_{0.5}\text{Ba}_{0.5-x}\text{Bi}_x\text{TiO}_3$ thin films were prepared by sol-gel route. The precursor solution was formed by appropriate ratios of barium, strontium, acetate and bismuth nitrate dissolved in glacial acetic acid to form solution A and titanium tetrabutoxide, acetylacetone and glycerin dissolved in ethanol to form solution B. Then solution A was mixed with solution B under stirring for sometime. Then the precursor solution was spin-coated onto Pt/ $\text{TiO}_2/\text{SiO}_2/\text{Si}(100)$ substrates. The films were spun at 3000 rpm for 60 s and were immediately dried in vacuum drying case and pyrolyzed at 200°C , and then heated at

*Author for correspondence (mse_fuxh@ujn.edu.cn)

750°C in an oven which was imbued with oxygen. The samples B₀, B₁, B₂, B₃, B₄, B₅ and B₆ had corresponding values of *x* which were 0, 0.007, 0.010, 0.015, 0.020, 0.025 and 0.030, respectively.

3. Microstructures and properties

Figure 1 shows the dielectric constant, ϵ_r , and dielectric loss, $\tan \delta$, as a function of Bi concentration in Sr_{0.5}Ba_{0.5-x}Bi_xTiO₃ measured by wide frequency LCR digital bridge, TH2816 at 1 kHz. It showed that Bi donor dependence of dielectric constant, ϵ_r , and dielectric loss, $\tan \delta$, decreased gradually with increasing Bi. This contributed to Ba²⁺ being substituted by Bi³⁺, and the dopant Bi³⁺ repressed the formation of oxygen vacancies, and reduced the agglomeration of vacancies in the interfacial region between the electrode and the substrate.

Figure 2 shows curves of temperature dependence of dielectric constant for Sr_{0.5}Ba_{0.5-x}Bi_xTiO₃ thin films. It also shows that the dielectric constant, ϵ_r , of the thin films

increased first with increasing temperature, and reached the maximum when temperature was at *T_m*, then ϵ_r decreased as the temperature was increased continuously. With the increasing donor Bi from B₀ to B₆, *T_m* peaks became wider, but the height became lower gradually which presented phase transition dispersion. In the meantime, *T_m* shifted to lower temperatures which could be explained by the bulk effects (Lei *et al* 2000) of BST crystal cells.

Dielectric constant showed scattering frequency characteristics due to the differences of response speeds (relaxation time) of each polarization mechanism in the electric fields. Figure 3 shows ϵ_r and $\tan \delta$ curves of Sr_{0.5}Ba_{0.5-x}Bi_xTiO₃ thin films measured by HP Agilent 4294A impedance analyser.

The dielectric constant decreased gradually with increasing frequency in the experimental frequency region (figure 3 (a)). Under low frequency, the directional reversal of dipole could catch up with the change of electrical fields, but dipole polarization could not catch up, when frequency increased to the relaxation time of the dipole, ϵ_r de-

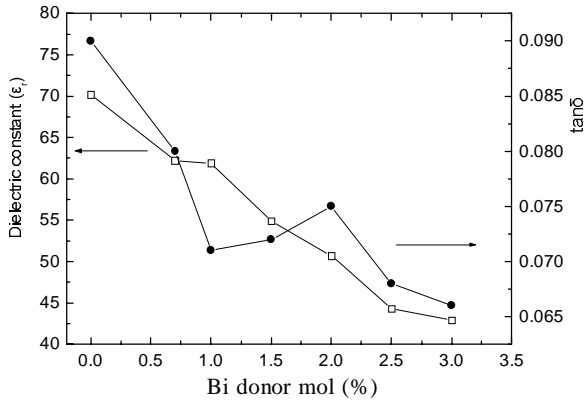


Figure 1. ϵ_r and $\tan \delta$ curves of Sr_{0.5}Ba_{0.5-x}Bi_xTiO₃ at 1 kHz.

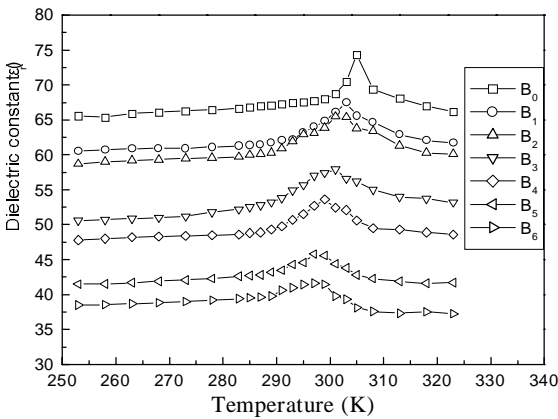


Figure 2. ϵ_r curves of Sr_{0.5}Ba_{0.5-x}Bi_xTiO₃ thin films with different temperatures.

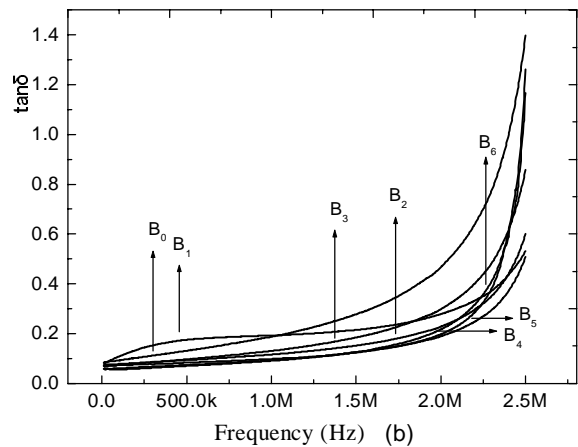
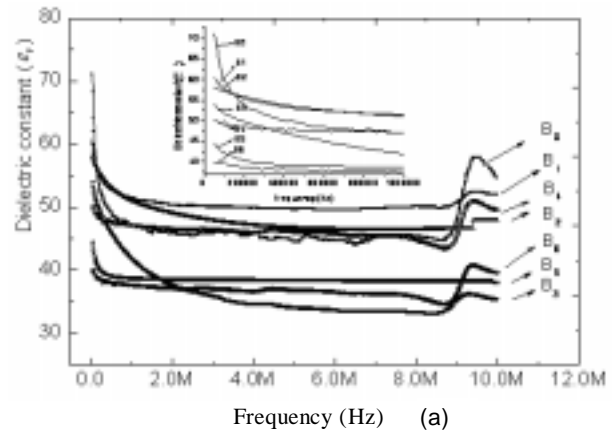


Figure 3. (a) ϵ_r and (b) $\tan \delta$ curves of Sr_{0.5}Ba_{0.5-x}Bi_xTiO₃ thin films at different frequencies.

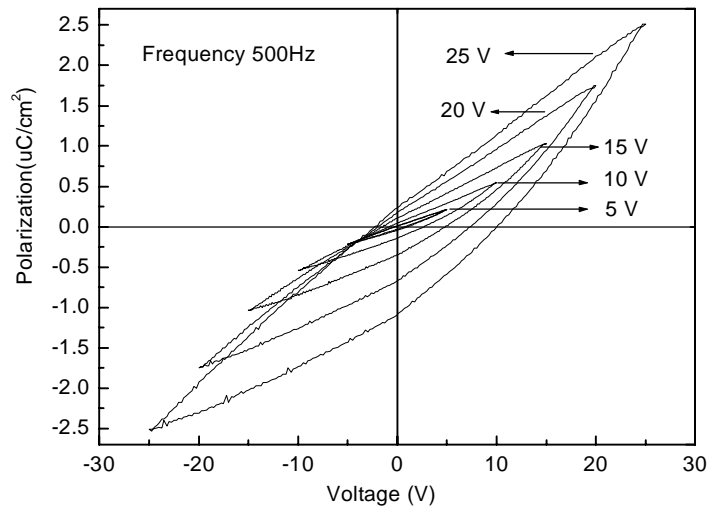


Figure 4. P - V hysteresis loops of B_1 thin films annealed on the Pt/TiO₂/SiO₂/Si (100).

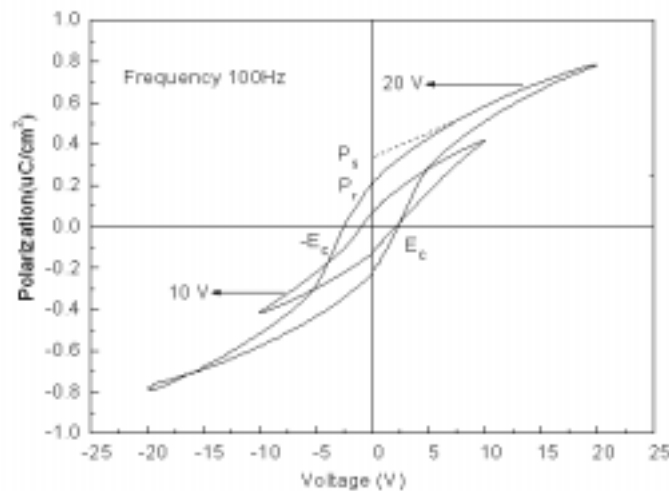


Figure 5. P - V hysteresis loops of B_3 thin films annealed on the Pt/TiO₂/SiO₂/Si (100).

creased. As frequency was above 8 MHz, dielectric constant, ϵ_r , had changed abruptly and gone through a maximum around 9.5 MHz for all the samples except B_5 . In the test frequency region, dielectric constants for B_1 and B_4 changed less, so B_1 and B_4 have better scattering frequency characteristics.

In figure 3(b), the dielectric loss, $\tan \delta$, increased gradually with increasing frequency, and in the frequency range of 10^3 – 10^6 Hz, dielectric loss increased slowly, but increased dramatically as frequency was above 2 MHz. This is mainly because of the reversal of spontaneous polarization of thin films under the applied fields. The higher the frequency, the more the energy is needed when

spontaneous polarization reversal overcomes the space barrier, and the dielectric loss, $\tan \delta$, increases with increasing frequency. When frequency gets below 2 MHz, all other samples (except B_0 and B_1) changes little which shows that the scattering frequency characteristics of $\tan \delta$ for thin films improved when Bi was doped.

There is relatively not much literature on the ferroelectric properties of BST thin films prepared by the sol-gel process. The main reason is that the grain sizes of fabricated BST thin films by sol-gel process are very small, generally below 70 nm, while that of polycrystal BST thin films with ferroelectric properties are above 120 nm. Also with the increase of Sr, the c/a ratio decreases

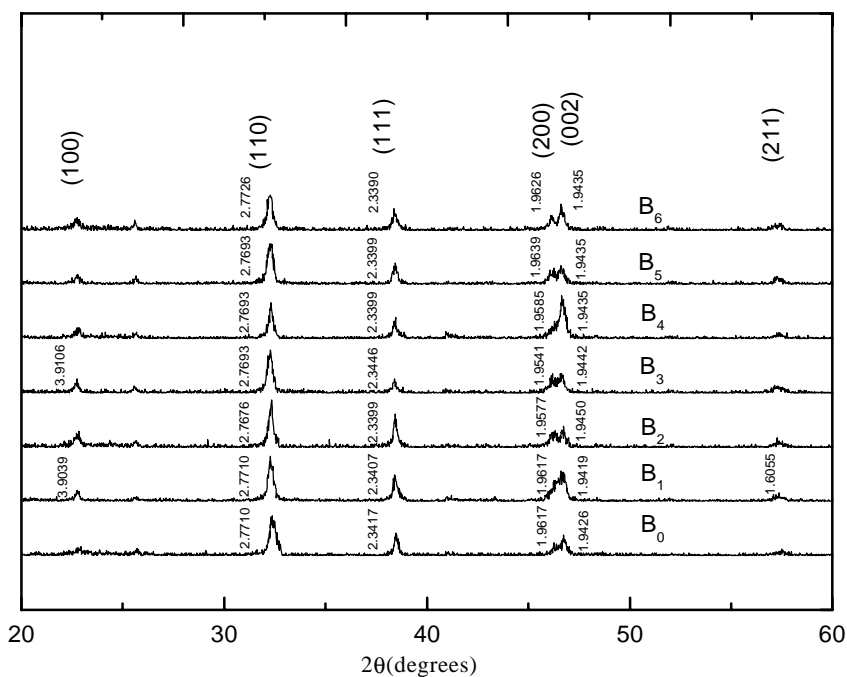


Figure 6. XRD patterns of $\text{Sr}_{0.5}\text{Ba}_{0.5-x}\text{Bi}_x\text{TiO}_3$ thin films annealed at 750°C for 1 h.

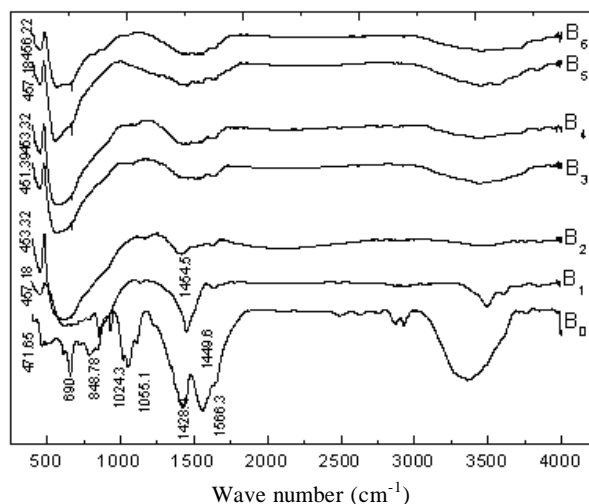


Figure 7. FTIR patterns of BST powders with different contents.

gradually, which leads to the diminishing of spontaneous polarization. The hysteresis loops of B_1 and B_3 thin films on TFA analyser 2000 Tester (made in Germany) was obtained, and the results are shown in figures 4 and 5.

In figures 4 and 5, the saturable extent of B_3 in which more dopant Bi was added, was obviously better than that

of B_1 . Figure 4 shows that at 500 Hz the hysteresis loop becomes fatter with increasing voltage, the remnant polarization (P_r) and coercive field (E_c) increases obviously, but they were observed in the positive direction of x -axis and the negative direction of y -axis at the same time. Figure 5 shows that at 100 Hz and 20 V, the remnant polarization (P_r), spontaneous polarization (P_s) and coercive field (E_c) of thin film B_3 was $0.22 \mu\text{C}/\text{cm}^2$, $0.32 \mu\text{C}/\text{cm}^2$ and $60 \text{ kV}/\text{cm}$, respectively.

XRD pattern of $\text{Sr}_{0.5}\text{Ba}_{0.5-x}\text{Bi}_x\text{TiO}_3$ thin films, $B_0 \sim B_6$, annealed at 750°C for 1 h, is shown in figure 6. This pattern is indexed to a tetragonal perovskite cell. The evolution of (200) and (002) reflections, which are the characteristics of tetragonal BST, was monitored. It indicates that a little dopant, Bi^{3+} , did not alter the perovskite, and cation, Bi^{3+} , may stay in the perovskite lattice by means of substitution. The electron configuration of cation Bi^{3+} is $5d^{10}6s^26p^0$, $5d$ orbit is full, so the octahedral energy level is much lower than that of Ti^{4+} ($3d^04s^0$), and the stability energy of Bi forming the centre of octahedron is smaller than that of Ti, so the cation Bi^{3+} substituted the sites of Ba in the perovskite lattice.

In order to investigate the influence of Bi on Ti–O and octahedron $[\text{TiO}_6]$, the gel with dopant Bi was heated in the oven at 900°C , and then analysed on FTS165 infrared analyser, the spectrum is shown in figure 7.

In figure 7, the peak at 471.65 cm^{-1} , is an octahedron $[\text{TiO}_6]$ characteristic absorption peak, the peaks at this

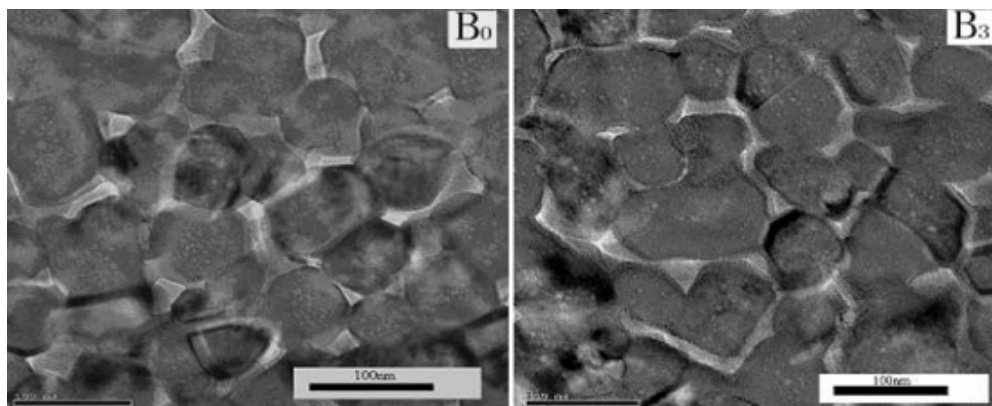


Figure 8. TEM micrographs of B_0 and B_3 .

position have shifted towards the direction of the lower wave-numbers from B_0 to B_6 , into which more dopant Bi^{3+} was added.

Because the dopant, Bi^{3+} , necessarily affects the reciprocity with surrounding cations, the surroundings of Bi^{3+} in the perovskite structure is the same as those of Ba^{2+} , i.e. they are all surrounded by eight Ti–O octahedrons, cation Bi^{3+} is much easier to shift and deviates from central position than cation Ba^{2+} or Sr^{2+} . So when the temperature gets high to crystallize, the vibration frequency and fluctuations all changed and that resulted in the shift of wave number.

The presence of carbonate absorption bands (1428, 848, 690 cm^{-1} etc) appearing in spectrum B_0 (figure 7), indicated that the minor phase(s) of barium carbonate and strontium carbonate coexisted in powder B_0 , while with the increasing donor Bi from B_0 to B_6 , the amount of minor phase(s) decreased.

TEM micrographs (figure 8) of B_0 and B_3 on JEM-2010TEM helps us to judge precisely the grain sizes. The average grain sizes for B_0 are 90 nm, and B_3 , 70 nm. Abnormal growth was seen when dopant Bi was added.

4. Conclusions

$Sr_{0.5}Ba_{0.5-x}Bi_xTiO_3$ ($x \leq 0.030$ mol) thin films were fabricated by sol–gel technique. The microstructure and properties of thin films affected by the dopant, Bi^{3+} , are as follows:

- (I) Dielectric loss improved as dopant Bi^{3+} increased, but dielectric constant decreased at the same time. The temperature, T_m , tends to decrease with increase of dopant Bi^{3+} , and the T_m peak positions tend to lower. The scattering frequency characteristics of dielectric constant, ϵ_r , and dielectric loss, $\tan \delta$, also improved.
- (II) The Bi^{3+} substituted phase was tetragonal perovskite. The infrared characteristic absorption peak of octahedron [TiO₆] shifted towards lower wave numbers which led to loss of chemical bonds.

Acknowledgement

We thank the foundation of Jinan University for support.

References

- Erker E G, Nagra A S, Liu Y, Periaswamy P, Taylor T R, Speck J and York R A 2000 *IEEE Microwave and Guided Wave Lett.* **10** 10
- Kotecki D E *et al* 1999 *IBM J. Res. Dev.* **43** 367
- Liou J W and Chiou B S 1997 *Mater. Chem. & Phys.* **51** 59
- Liu Y, Borgioli A and Nagra A S 2000 *IEEE Microwave and Guided Wave Lett.* **10** 415
- Lei Zhang, Weilie Zhong, Yiping Peng and Yuguo Wang 2000 *J. Appl. Phys.* **49** 1371
- Mandelelman J A, Dennard R H, Bronner G B, DeBrosse J K, Divakaruni R, Li Y and Radens C J 2002 *IBM J. Res. & Dev.* **46** 187